Title

Pharmacokinetic Model of Tenofovir and Emtricitabine and Their Intracellular Metabolites in Patients in the ANRS 134-COPHAR 3 Trial Using Dose Records.

Journal

Antimicrobial Agents and Chemotherapy, 67(5)

Authors

Bertrand, Julie
Barrail-Tran, Aurélie
Fayette, Lucie
et al.

Publication Date

2023-05-17

DOI

10.1128/aac.02339-18

Peer reviewed

AMERICAN SOCIETY FOR MICROBIOLOGY | Antimicrobial Agents and Chemotherapy®

ANTIVIRAL AGENTS

Pharmacokinetic Model of Tenofovir and Emtricitabine and Their Intracellular Metabolites in Patients in the ANRS 134-COPHAR 3 Trial Using Dose Records

Julie Bertrand,[a] Aurélie Barrail-Tran,[b,c] Lucie Fayette,[a] Rada Savic,[d] Cécile Goujard,[e,f] Elina Teicher,[e] Caroline Barau,[g] Alain Pruvost,[h] Anne-Marie Taburet,[b,c] France Mentré,[a] Céline Verstuyft,[f,i] on behalf of the ANRS 134-COPHAR 3 trial group

[a]UMR 1137, IAME, INSERM, Université Paris Cité, Paris, France
[b]AP-HP, Hôpital Bicêtre, Pharmacie Clinique, Le Kremlin-Bicêtre, France
[c]UMR 1184, Center for Immunology of Viral Infections and Autoimmune Diseases, INSERM, Université Paris Sud, Paris, France
[d]Department of Bioengineering and Therapeutic Sciences, University of California San Francisco, San Francisco, California, USA
[e]AP-HP, Hôpital Bicêtre, Service de médecine interne et d'immunologie clinique, Le Kremlin-Bicêtre, France
[f]CESP, Team Epidémiologie Clinique, INSERM UMR 1018, Faculté de Médecine, Univ Paris-Saclay, Le Kremlin Bicêtre, France
[g]AP-HP, Hôpital Henri Mondor, Plateforme de Ressources Biologiques, Créteil, France
[h]Département Médicaments et Technologies pour la Santé, SPI, CEA, INRAE, Université Paris Saclay, Paris, France
[i]AP-HP, Hôpital Bicêtre, Service de génétique moléculaire et pharmacogénétique, Le Kremlin-Bicêtre, France

ABSTRACT Tenofovir (TFV) and emtricitabine (FTC) are part of the recommended highly active antiretroviral therapy (ART). Both molecules show a large interindividual pharmacokinetic (PK) variability. Here, we modeled the concentrations of plasma TFV and FTC and their intracellular metabolites (TFV diphosphate [TFV-DP] and FTC triphosphate [FTC-TP]) collected after 4 and 24 weeks of treatment in 34 patients from the ANRS 134-COPHAR 3 trial. These patients received daily (QD) atazanavir (300 mg), ritonavir (100 mg), and a fixed-dose combination of coformulated TFV disoproxil fumarate (300 mg) and FTC (200 mg). Dosing history was collected using a medication event monitoring system. A three-compartment model with absorption delay (T_{lag}) was selected to describe the PK of, respectively, TFV/TFV-DP and FTC/FTC-TP. TFV and FTC apparent clearances, 114 L/h (relative standard error [RSE] = 8%) and 18.1 L/h (RSE = 5%), respectively, were found to decrease with age. However, no significant association was found with the polymorphisms *ABCC2* rs717620, *ABCC4* rs1751034, and *ABCB1* rs1045642. The model allows prediction of TFV-DP and FTC-TP concentrations at steady state with alternative regimens.

KEYWORDS pharmacokinetics, pharmacogenetics, antiretroviral, HIV, mixed-effect models, nonlinear models

Tenofovir (TFV) with lamivudine or emtricitabine (FTC) is the recommended nucleos(t)ide reverse transcriptase inhibitor backbone in combination with a third antiretroviral (ARV) drug for the treatment of naive patients living with HIV (PLWHIV) or pre-exposure prophylaxis (PrEP) (1). Both TFV and FTC are nucleos(t)ides, and their active intracellular forms, TFV-diphosphate (TFV-DP) and FTC-triphosphate (FTC-TP), hinder the activity of HIV reverse transcriptase and prevent the production of new virions by competing with natural substrates.

TFV pharmacokinetics (PK) has been modeled for the last 20 years in healthy volunteers, PLWHIV, or both (2), while fewer data are available for FTC PK (3). Recently, models have focused on describing TFV and TFV-DP and/or FTC and FTC-TP concentrations (4, 5). Such combined PK models have been previously coupled with simulations from a mathematical model of viral load (6) and with a pharmacodynamic model of binding to the HIV reverse transcriptase natural substrates (7). These studies made it possible to define target

Address correspondence to Julie Bertrand, julie.bertrand@inserm.fr.

The authors declare no conflict of interest.

Received 5 November 2018
Returned for modification 7 December 2018
Accepted 22 March 2023
Published 26 April 2023

concentrations for TFV-DP and FTC-TP prevention of cell infection and inhibition of the production of endogenous deoxynucleoside triphosphates. Studies on TFV PK focusing on PrEP yielded data and models which are not readily transferable to PLWHIV in terms of virological success (8–10), and no consensus has been reached with regard to the concentration needed to reach an optimal virologic response to HIV antiretroviral treatment (ART).

Some of these studies also identified factors to explain the interindividual variability in the PK of TFV, TFV-DP, FTC, and FTC-TP, but a high degree (coefficient of variation $>$ 50%) of unexplained variability remains. The *ABCC2* and *ABCC4* genes encode two members of the ATP-binding cassette transporters ensuring cellular uptake and excretion, MRP2 and MRP4, respectively. TFV is a known substrate of MRP4 but not of MRP2 (11). However, the genetic polymorphism *ABCC2* (rs717620) has a functional effect associated with a decrease in tenofovir-induced kidney tubular dysfunction (12). Moss et al. attribute this effect to an endogenous substrate for MRP2, either enhancing TFV toxicity or competing with TFV for excretion by MRP4 (13). The genetic polymorphism *ABCC4* (rs1751034) is a synonymous polymorphism which was associated with reduced expression/function in a small pilot study (14) and consequently with increased TFV concentrations (15, 16) and TFV-DP intracellular concentrations (17). The ABCB1 transporter (P-glycoprotein [P-gp]) is an efflux transporter ubiquitously expressed in the human body. TFV prodrug is a substrate (18), and the TFV cerebrospinal fluid-to-plasma ratio has been linked to *ABCB1* polymorphism, although not withstanding multiple test correction (19). There are several genetic polymorphisms in *ABCB1*; here, we focused on the rs1045642, which is the most frequently studied and associated with a modification of the expression and activity of the P-gP (20, 21). As for FTC, the genetic polymorphism *ABCC2* (rs154962860) was associated with significantly increased concentrations in women (22).

The ANRS 134-COPHAR 3 trial was a multicenter prospective trial conducted in 35 HIV-1-infected, treatment-naive patients who received atazanavir-ritonavir (300/100 mg) combined with tenofovir disoproxil fumarate-emtricitabine (300/200 mg) in a fixed-dose combination. The primary objective was to assess the PK/pharmacogenetics of atazanavir administered with ritonavir, using adherence rates as measured by a medication event monitoring system (MEMS) (23). Modeling the atazanavir and ritonavir concentrations, Savic et al. (23) showed that the use of exact dosing data lowers the interoccasion variability of oral clearance, leading to reliable parameter estimates and a stable estimation procedure. PK of TFV and FTC have not yet been analyzed in this trial. More recently, several attempts have been made to lower drug exposure in patients on maintenance therapy, in order to limit long-term ARV toxicity, and data generated on TFV and FTC were of particular interest, as these two drugs remain part of the gold standard of ARV regimens. In particular, the ANRS 170-QUATUOR trial showed the noninferiority of a 4-day-a-week maintenance regimen relative to a standard continuous ART triple therapy over 48 weeks in 636 participants (24).

In the present work, we built a PK model of TFV and its intracellular metabolite concentrations on one side and FTC and its metabolite concentrations on the other side, using concentrations collected for patients included in the ANRS 134-COPHAR 3 trial with exact dosing data, aiming to explore covariates, including genetic polymorphism, explaining their interindividual variability. Using this model, we simulated TFV/TFV-DP and FTC/FTC-TP exposures for a 4- and a 7-day-a-week dosing regimen to be compared with target concentrations for virologic response from the literature.

RESULTS

Data. Of the 35 subjects included in the ANRS 134-COPHAR 3 clinical trial, 34 provided data for the present analysis, as concentrations were missing for one patient. Patients' demographic characteristics are given in Table 1, and information on genetic polymorphisms is given in Table 2.

Raw adherence data indicated overall good adherence to the TFV-FTC fixed-dose combination in the studied population, with a majority of the prescribed doses being taken as prescribed: median, 94% (range, 47 to 100). Discrepancies between MEMS-recorded and patient-reported intake prior to sampling occurred only six times. There was no plasma

TABLE 1 Characteristics of the 34 patients analyzed in the study of tenofovir and emtricitabine concentrations in the ANRS 134-COPHAR 3 trial

Characteristic	Value
Wt (kg) [median (range)]	71.0 (42.0–91.0)
Age (yr) [median (range)]	38.5 (26.0–68.0)
Creatinine clearance (mL/min) [median (range)]	100.8 (50.9–158.5)
Atazanavir clearance (L/h) [median (range)]	6.8 (3.8–15.0)
Gender (women/men) [no. (%)]	6 (17)/28 (82)
Nationality (Caucasian/African) [no. (%)]	23 (67)/11 (32)

concentration below the lower limit of quantification (LLOQ), and 3 intracellular samples exhibited chromatographic issues or cell counts below the LLOQ and were discarded. In total, there were 225 plasma and 17 intracellular concentrations analyzed for both tenofovir and emtricitabine (Fig. 1). Of note, the three highest intracellular concentration values at week 24 are not trough concentrations but were collected less than 5 h post-administration.

Pharmacokinetic model. A three-compartment model with absorption delay (T_{lag}) was selected to describe the PK of TFV/TFV-DP and the PK of FTC/FTC-TP (Fig. 2). Both TFV and FTC diffused in a central and a peripheral compartment with a nonlinear uptake from the plasma central compartment into a cell compartment to become TFV-DP and FTC-TP, respectively (25). As only one sampling time was collected for the cellular concentrations per occasion, we fixed K_m (Michaelis-Menten constant) and K_{em} (elimination rate constant from the cell) at 0.946 μg/mol/L and 0.0176/h (25) and 0.102 μg/mol/L and 0.006/h (26) for FTC-TP and TFV-DP, respectively.

Model parameter mean values and interindividual coefficient of variation estimates with their relative standard errors are given in Table 3 for the models with and without covariates. Interindividual variability was negligible for apparent central compartment of distribution V_c/F_{FTC}, apparent peripheral compartment of distribution V_p/F_{FTC}, V_c/F_{TFV}, and apparent intercompartmental clearance Q/F_{TFV}. Apparent elimination clearance CL/F_{FTC} and Q/F_{FTC} were found to be correlated ($r = 0.76$, $P = 0.0023$) as well as CL/F_{TFV} and V/F_{TFV} ($r = 0.78$, $P = 0.0015$). Interoccasion variability was negligible. Shrinkage was below 50% except for the maximum rate of entrance into the cell for TFV-DP $V_{max\_TFV\text{-}DP}$ (72%) and $V_{max\_FTC\text{-}TP}$ (76%).

After covariate model building, no significant association was found with the genetic polymorphisms under study, and CL/F_{TFV} was found to decrease with age (Wald test P value = 0.0073), as well as CL/F_{FTC} ($P = 0.0059$), and V_p/F_{TFV} ($P = 0.0014$). The covariate model visual predictive checks were overall satisfactory (Fig. 3).

Model predictions and simulations. Among the patients enrolled in the ANRS 134-COPHAR 3 trial, 30 experienced successful viral suppression at week 24 (plasma HIV RNA $<$ 40 copies/mL). The average concentration (C_{avg}) and minimum concentration (C_{min}) estimates according to dosing history are displayed in Table 4 for TFV, TFV-DP, FTC, and FTC-TP. Among the five patients with detectable viral load levels at week 24, four had TFV-DP and FTC-TP C_{avg} below the median estimates of 136 fmol/10^6 cells and 8 pmol/10^6 cells, respectively.

As shown in Fig. 4, according to model simulations, the change in concentration profiles at steady state between a regimen of 4 consecutive days a week (4D) and one of 7 days a week (7D) is different between FTC-TP and TFV-DP in terms of C_{min} but not of C_{avg}. Indeed,

TABLE 2 Genetic polymorphisms in the 34 patients analyzed in the study of tenofovir and emtricitabine concentrations in the ANRS 134-COPHAR 3 trial

	Caucasian		African[b]	
Polymorphism	No. (%)	P^a	No. (%)	P^a
ABCC2 rs717620 CC/CT	14 (60)/9 (30)	0.49	7 (70)/3 (30)	0.76
ABCC4 rs1751034 AA/AG/GG	16 (70)/7 (30)/0 (0)	0.64	3 (30)/5 (50)/2 (20)	0.97
ABCB1 rs1045642 CC/CT/TT	6 (26)/11 (48)/6 (26)	0.83	6 (60) /3 (30)/1 (10)	0.53

[a]*P*, Hardy-Weinberg equilibrium *P* value.
[b]One of the 11 African patients had no genotype information available.

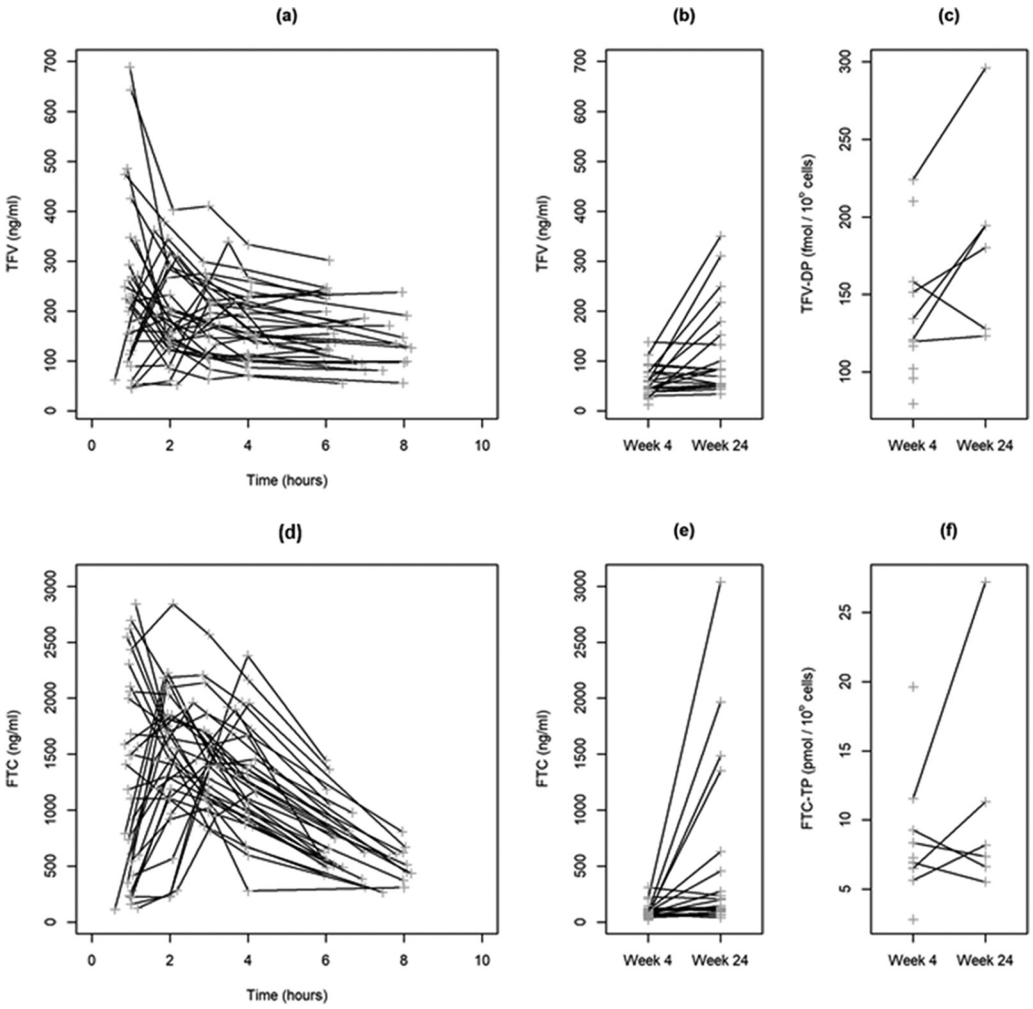

FIG 1 Profiles of observed (gray plus signs) TFV and FTC concentrations versus time since last dose sampled in clinic at week 4 (a and d) plus predose concentrations at week 4 and 24 (b and e) and TFV-DP and FTC-TP concentrations at weeks 4 and 24 (c and f) for the 34 analyzed patients included in the ANRS 134-COPHAR 3 trial and receiving a fixed-dose combination of coformulated tenofovir disoproxil fumarate (300 mg) and emtricitabine (200 mg).

considering the median predicted percentiles at steady state over a 2-week window, the C_{min} varies between the 7D and 4D regimens from 8 to 3 pmol/10^6 for FTC-TP (ratio of 2.6) and from 143 to 89 fmol/10^6 cells for TFV-DP (ratio of 1.6), while C_{avg} varies similarly between the 7D and 4D regimen from 8 to 5 pmol/10^6 cells for FTC-TP (i.e., a ratio of 1.6) and from 146 to 101 fmol/10^6 cells for TFV-DP (i.e., a ratio of 1.4). Among the five patients with detectable viral load levels at W24 in the ANRS 134-COPHAR 3 trial, four had TFV-DP and FTC-TP C_{avg} below the median C_{avg} estimates for a 7D regimen. For two of them, the TFV-DP and FTC-TP C_{avg} were even below the median C_{avg} estimates for a 4D regimen.

DISCUSSION

In the present work, we modeled the plasma TFV and FTC concentrations, as well as the intracellular TFV-DP and FTC-TP concentrations, in 34 patients of the ANRS 134-COPHAR 3 trial, controlling for their adherence with a MEMS. Our model identified the predictive value of age for the average concentrations of FTC and TFV in the plasma and at the target site. Considering the adherence data collected in the ANRS 134-COPHAR 3 trial, the model makes it possible to derive lower limits for TFV-DP and FTC-TP average concentrations contributing to viral suppression within combined ART.

Our estimates of clearances and volumes for TFV compared well to previously reported values except for Q/F_{TFV}, which was almost at twice the upper end of the range (2, 26).

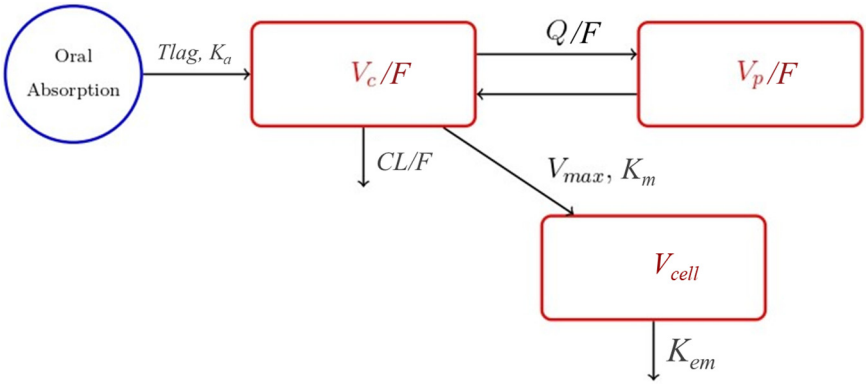

FIG 2 Schema of the pharmacokinetic model selected to describe the pharmacokinetics of TFV, TFV-DP, FTC, and FTC-TP in the ANRS 134-COPHAR 3 trial. T_{lag}, absorption delay; K_a, absorption rate constant; CL/*F*, apparent elimination clearance; V_c/F, apparent central compartment of distribution; *Q*/*F*, apparent intercompartmental clearance; V_p/F, apparent peripheral compartment of distribution; K_{em}, elimination rate constant from the cell; V_{max}, maximum rate of entrance into the cell; K_m, Michaelis-Menten constant; V_{cell}, volume of the cellular compartment (assuming the volume of a PBMC to be approximately 0.2 pL).

Similarly, our parameters for FTC, based on less abundant literature, were in agreement with the literature (27, 28). This translates to terminal half-life estimates of 18.8 h for TFV and 21.3 h for FTC, in the middle of the values reported in the literature for TFV (from 11.6 to 31.0 h) and FTC (from 3.0 to 40.5 h), as summarized by Chen et al. (7).

The long half-life of TFV-DP (115 h, as estimated in reference 26) means that a steady state of concentrations will be reached on average a month or more after treatment initiation (29). Our first peripheral blood mononuclear cell (PBMC) sample was drawn at week 4 after ARV initiation and the second sample at week 24, at the end of the study. There is a trend toward a slightly increased concentration between these 2 samples, meaning that a steady state was nearly reached at week 4 in most patients, supporting higher intracellular concentrations than in previous studies. In addition, higher concentrations of TFV have been reported in some studies when tenofovir disoproxil fumarate (TDF) was coadministered with ritonavir-boosted protease inhibitors, such as lopinavir or atazanavir (30), but not in others (17). Ritonavir and lopinavir inhibit relevant transporters SLC22A8 and MRP4 *in vitro*, and a transporter-mediated drug interaction in the kidneys may explain the elevated TFV concentrations when these drugs are used (31). However, polymorphisms in *SLC22A6* (rs4149170 and rs11568626) have been analyzed and were not found to be associated with kidney toxicity or alteration in TFV renal clearance (13). Further, there is evidence that genetic polymorphisms of these transporters are not associated with the pharmacokinetics of several drugs, including TFV (15). Only one study compared the TFV-DP concentrations when TDF was combined with different ARV regimens. The reported C_{last} was 129 (27 to 945) fmol/10^6 cells when TDF was combined with a nonnucleoside reverse transcriptase inhibitors (NNRTI) and 188 (25 to 497) fmol/10^6 cells when TDF was combined with ritonavir-boosted lopinavir, again showing huge interindividual variability and suggesting that this drug-drug interaction may not have clinically relevant consequences for efficacy (32).

Age was found to decrease FTC clearance and TFV clearance and peripheral volume. Interestingly, TFV-DP and FTC-TP concentrations were found to be associated with age in another study (33). We did not find creatinine clearance effects on TFV and FTC clearances, as reported in references 15 and 34–37 and in references 27 and 38, respectively. Moreover, no effect of genetic polymorphisms was detected, although several genetic models were considered.

This is one of the few studies reporting intracellular concentrations of both TFV-DP and FTC-TP at steady state in PLWHIV whose adherence was well controlled. Studies have attempted to estimate the concentration of TFV-DP to be reached for preventing HIV acquisition in PrEP studies. Such a target was estimated to be 267 fmol/10^6 by Duwal et al. (6). For viral suppression, Chen et al. reported concentrations as high as 1,020 fmol/10^6 cells

TABLE 3 Parameter estimates for the basic and covariate model of tenofovir and emtricitabine concentrations collected in 34 patients of the ANRS 134-COPHAR 3 trial[a]

	Base model		Covariate model	
Parameter (unit)	**Estimate**	**RSE (%)**	**Estimate**	**RSE (%)**
Population values				
$T_{lag\ TFV}$ (h)	0.348	32	0.337	40
$K_{a\ TFV}$ (h)	2.45	32	2.25	33
CL/F_{TFV} (L/h)	114	8	228	27
$\beta_{CL/F_{TFV,age}}$			−0.017	38
V_c/F_{TFV} (L)	398	12	381	14
Q/F_{TFV} (L/h)	811	8	781	11
V_p/F_{TFV} (L)	1420	11	4570	46
$\beta_{Vp/FTFV,age}$			−0.029	40
$V_{max\ TFV\text{-}DP}$ (μmol/L/h)	0.006	10	0.006	10
$K_{m\ TFV\text{-}DP}$ (μmol/L)	0.102	Fixed	0.102	Fixed
$k_{em\ TFV\text{-}DP}$ (h)	0.006	Fixed	0.006	Fixed
$T_{lag\ FTC}$ (h)	0.421	26	0.377	30
$K_{a\ FTC}$ (h)	1.37	21	1.45	23
CL/F_{FTC} (L/h)	18.1	5	28.0	16
$\beta_{CL/FFTC,age}$			−0.010	35
V_c/F_{FTC} (L)	75.9	5	75.2	5
Q/F_{FTC} (L/h)	4.48	21	46	16
V_p/F_{FTC} (L)	121	21	120	18
$V_{max\ FTC\text{-}TP}$ (μmol/L/h)	1.42	17	1.49	17
$K_{m\ FTC\text{-}TP}$ (μmol/L)	0.946	Fixed	0.946	Fixed
$k_{em\ FTC\text{-}TP}$ (h)	0.0176	Fixed	0.0176	Fixed
Interindividual coefficient of variation (%)				
$\omega T_{lag\ TFV}$	127	22	150	41
$\omega K_{a\ TFV}$	116	20	113	22
$\omega CL/F_{TFV}$	38	13	35	13
$\omega V_p/F_{TFV}$	57	15	50	17
$\omega V_{max\ TFV\text{-}DP}$	29	31	26	32
$\rho CL/F_{TFV}$, V_p/F_{TFV}	0.78[b]	11	0.73[b]	14
$\omega T_{lag\ FTC}$	116	18	122	20
$\omega K_{a\ FTC}$	83	19	90	19
$\omega CL/F_{FTC}$	28	15	24	14
$\omega Q/F_{FTC}$	82	27	63	21
$\omega V_{max\ FTC\text{-}TP}$	44	28	43	44
$\rho CL/F_{FTC}$, Q/F_{FTC}	0.76[b]	15	0.69[b]	20
Residual coefficient of variation (%)				
σTFV	16	7	15	NE
σTFV-DP	19	24	20	29
σFTC	20	9	20	8
σFTC-TP	30	31	28	26

[a]RSE, relative standard error; TFV, tenofovir (plasma concentrations); TFV-DP, tenofovir diphosphate (intracellular concentrations); FTC, emtricitabine (plasma concentrations); FTC-TP, emtricitabine triphosphate (intracellular concentrations); T_{lag}, time delay in absorption; K_a, absorption rate constant; CL/*F*, apparent elimination clearance; V_c/F, apparent central compartment of distribution; *Q*/*F*, apparent intercompartmental clearance; V_p/F, apparent peripheral compartment of distribution; V_{max}, maximal uptake rate constant; K_m, Michaelis-Menten constant; k_{em}, elimination rate constant from the cell; $\beta_{PK\ parameter,\ covariate}$, additive effect size of covariate on log PK parameter with a $\beta_{CL/FTFV,age}$ of −0.017 indicating CL/F_{TFV} decreases of 15 and 39% in patients 10 and 30 years older than the median age (38.5 years), a $\beta_{Vp/FTFV,age}$ of −0.029 indicating V_p/F_{TFV} decreases of 25 and 58%, and a $\beta_{CL/FFTC,age}$ of −0.010 indicating CL/F_{FTC} decreases of 10 and 26%; NE: not estimated due to numerical issue.
[b]Correlation estimates are not in percent.

and 44.4 pmol/10^6 cells for TFV-DP and FTC-TP, using an indirect response model (7), whereas Ma et al. (39) reported consistent TFV-DP 50% effective concentrations (EC_{50}) between *in vivo* (0.09 μmol/L ≈ 18 fmol/10^6 cells) and *in vitro* (0.26 μmol/L ≈ 52 fmol/10^6 cells) experiments. This consistency strengthens their use as targets in clinical care to accomplish maximal viral load suppression. However, such an estimate has yet to be provided for FTC-TP levels.

Our model allowed simulation of plasma and intracellular concentrations of TFV, TFV-DP, FTC, and FTC-TP with different drug regimens. This is important because in selected patients

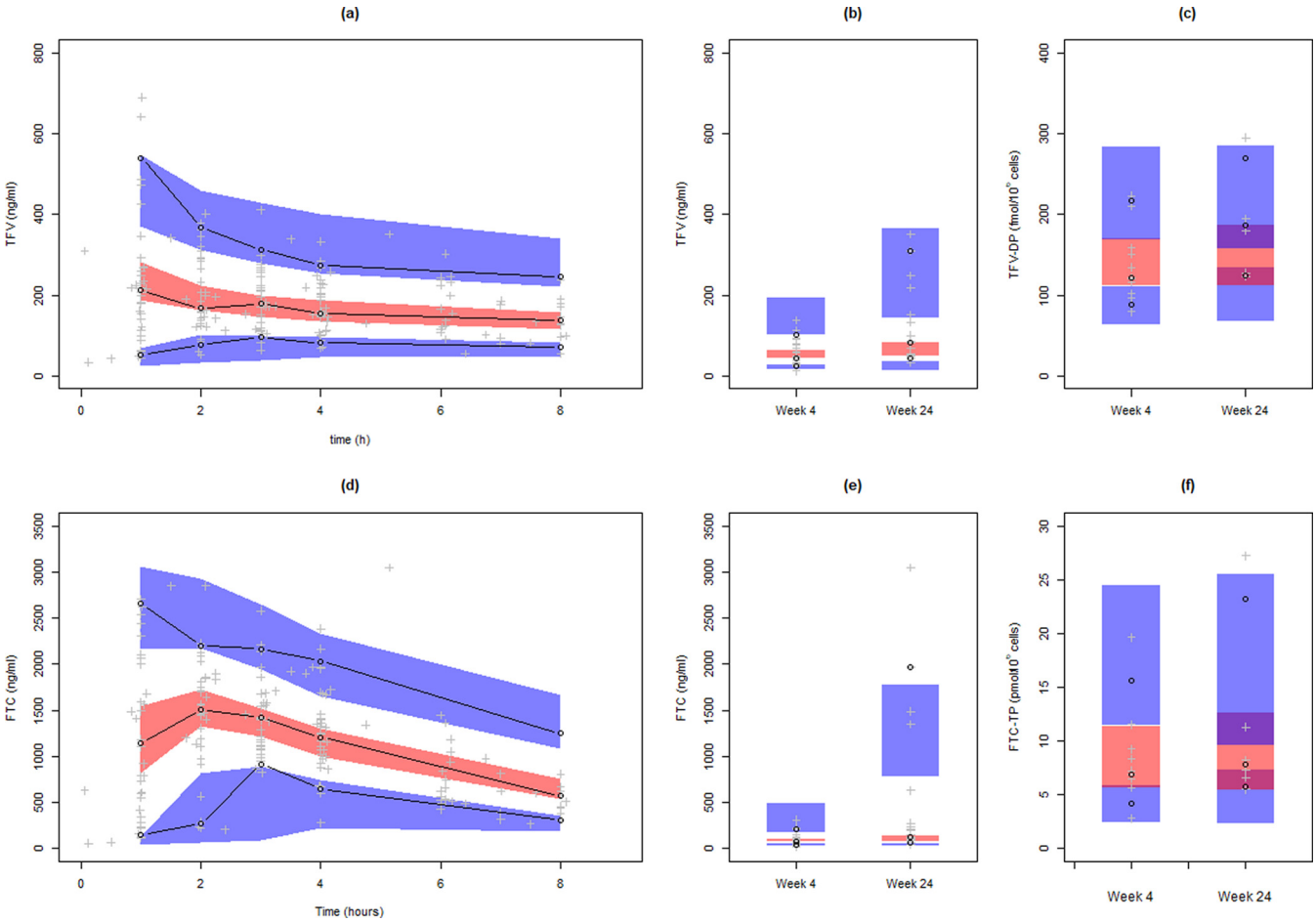

FIG 3 Visual predictive check plots using the combined model inclusive of all covariate effects for TFV and FTC profiles sampled in the clinic at week 4 (a and d), for the predose concentrations at weeks 4 and 24 (b and e), and for TFV-DP and FTC-TP concentrations at weeks 4 and 24 (c and f). The three bands represent the 90% confidence intervals around the 5th, 50th, and 95th predicted percentiles. The black dots and lines represent the 5th, 50th, and 95th observed percentiles.

on virological suppression, a reduced regimen could be an option. For instance, the BREATHER (PENTA 16) trial showed the noninferiority of maintaining virological suppression in children, adolescents, and young adults for short-cycle therapy versus continuous therapy at 48 weeks (40). Here, we considered the 4-day-a-week course of the ANRS 162 4D pilot study, where most patients were on efavirenz, with a long half-life (41), and the ANRS 170-QUATUOR study, where patients were on randomization stratified according to the family of the third antiretroviral agent (integrase inhibitor, protease inhibitor, or NNRTI) (24). Based

TABLE 4 Average and minimal concentrations as predicted from the covariate model for tenofovir (TFV), emtricitabine (FTC) and their metabolites (TFV-DP and FTC-TP)

Concentration	Regimen	Median (range) for: TFV (ng/mL)	TFV-DP (fmol/10^6 cells)	FTC (ng/mL)	FTC-TP (pmol/10^6 cells)
C_{avg}	ANRS 134-COPHAR 3[a]	99 (37–262)	136 (31–239)	413 (111–932)	8 (2–18)
	7 days/wk[b]	107 (45–265)	146 (91–239)	440 (208–922)	8 (4–18)
	4 days/wk[b]	61 (25–152)	101 (55–172)	251 (119–527)	5 (2–12)
C_{min}	ANRS 134-COPHAR 3[a]	28 (0–68)	125 (0–234)	54 (0–142)	6 (0–16)
	7 days/wk[b]	52 (15–130)	142 (88–234)	78 (25–248)	8 (3–17)
	4 days/wk[b]	1 (0–5)	8 (44–151)	11 (0–46)	3 (1–7)

[a]In the 34 patients of the ANRS 124-COPHAR 3 trial from W4 to the last observation, according to dosing history.
[b]In 1,000 subjects over a two-week window at steady state, assuming perfect adherence.

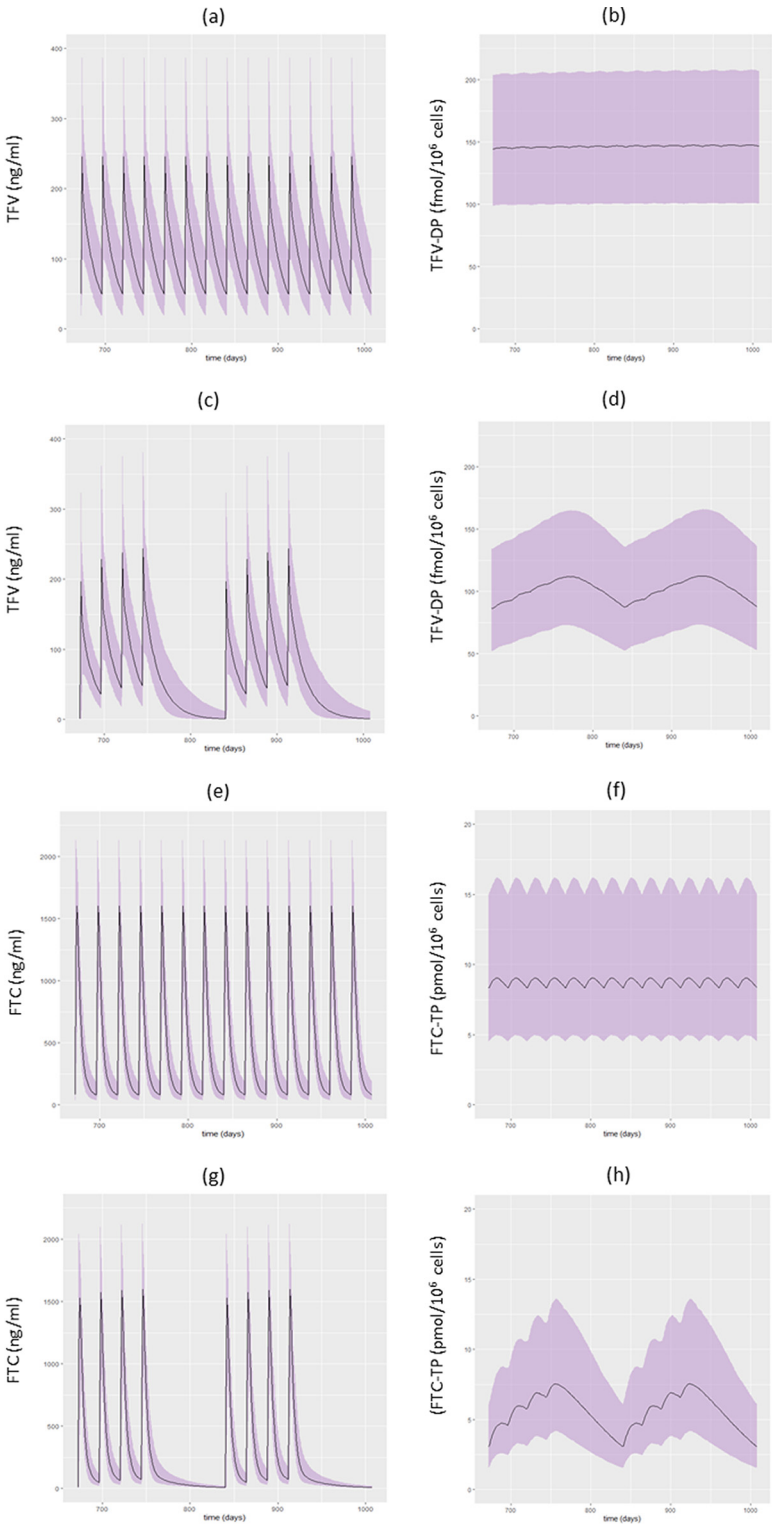

FIG 4 Prediction interval (80%, gray area) and median concentrations (black line) of TFV and TFV-DP with a 7-day-a-week regimen (7D) (a and b) and a 4-consecutive-day-a-week regimen (4D) (c and d) and FTC and FTC-TP concentrations with a 7D (e and f) and a 4D (g and h) regimen over 15 days at steady state based on a simulation from the model of 1,000 fully adherent patients.

on simulations for an intermittent maintenance regimen, TFV-DP concentration fluctuation was minimal, although average concentrations were obviously lower than with full doses in a continuous regimen. In contrast, as a consequence of a shorter intracellular half-life (39 h, as estimated in reference 25), FTC-TP fluctuations were important, and whether a lower nadir could be at risk of selecting resistant virus strains remains an issue, particularly if the third agent also has a short half-life.

The present work has several limitations. First, the number of patients certainly hindered the capture of factors explaining interindividual variability, and the number of intracellular samples prevented the estimation of all the parameters involved in the nonlinear entrance of TFV and FTC into the cell. Second, our results may not hold for tenofovir alafenamide fumarate (TAF), which is available in some high-income countries as a noninferior alternative to TDF, prescribed at a much lower dosage (42) and with a lower incidence of adverse effects in the first clinical trials, possibly due to low TFV plasma concentrations. However, the long-term consequences of higher TFV-DP concentrations after TAF administration still need to be assessed (43). Third, we did not have concentration data from the ANRS 170-QUATUOR study to overlay on our simulation graphs. Finally, these data are observational, so the suggested link between C_{avg} estimates and viral load suppression should be considered with caution.

Despite those limitations, our study provides unique data on TFV and FTC plasma concentrations and intracellular concentrations of their active phosphorylated active metabolites in PLWHIV, which were used to obtain model-derived exposure metrics accounting for gold standard adherence data. Further, the model and its population parameter estimates were used to provide exposure predictions supporting an intermittent dosing regimen in this population.

MATERIALS AND METHODS

Patients and study design. (i) Clinical trial. The ANRS 134-COPHAR 3 trial occurred in 2008 and included 35 treatment-naive patients who were started on a once-a-day treatment containing 300 mg of atazanavir boosted with 100 mg of ritonavir and a fixed-dose combination of coformulated nucleoside analogs: tenofovir disoproxil fumarate (300 mg) and emtricitabine (200 mg). The patients were followed for 24 weeks. Treatment success was defined as undetectable viral load levels (<40 copies/mL) at week 24. Reyataz (ATV) and Truvada (tenofovir disoproxil fumarate and emtricitabine) were kindly provided by Bristol-Myers Squibb and Gilead, respectively. More details are available in reference 23.

(ii) Pharmacokinetic data. Blood samples were collected from the subjects at weeks 4 and 24. During each visit, the patients were asked to report the exact time at which they had taken the last dose on the previous day. At week 4, a trough blood sample was collected, followed by administration of the drug and then collection of five additional samples, at 1, 2, 3, 4, and 8 h after the dose. At week 24, only a trough sample was collected. Overall, therefore, there were 7 samples for each subject over a 6-month period.

Plasma drug concentrations of TFV and FTC were determined in all 7 samples at the Bicêtre Hospital laboratory using a validated liquid chromatography-tandem mass spectrometry (LC-MS/MS) assay (44). The limit of quantification was 5 ng/mL. Intracellular concentrations of TFV-DP and FTC-TP were measured in the isolated PBMCs only before drug intake at weeks 4 and 24, by LC-MS/MS at the French Atomic Energy Commission (CEA) in Paris Saclay University according to a previously described method (45). For TFV-DP, within-assay reproducibility ranged from 88.4% to 108% and from 4.6 to 10.3% for accuracy and precision, respectively. Between-assay reproducibility ranged from 96% to 103% and from 3.4 to 10.4% for accuracy and precision, respectively. The calibration curve ranged from 100 to 7,000 fmol/sample (i.e., 10 to 700 fmol/10^6 cells for a sample pellet containing 10^7 cells). For FTC-TP, within-assay reproducibility ranged from 94.8 to 112.4% and from 0.6 to 3.2% for accuracy and precision, respectively. Between-assay reproducibility ranged from 93.8 to 114.6% and from 1.6% to 4% for accuracy and precision, respectively. The calibration curve ranged from 0.77 to 200 pmol/sample (i.e., 0.077 to 20 pmol/10^6 cells for a sample pellet containing 10^7 cells).

For the present study, plasma and intracellular concentrations were transformed to moles per liter, considering that 1 mol of emtricitabine and tenofovir is equal to 247 and 287 g, respectively, and the volume of a PBMC is approximately 0.2 pL (46, 47).

(iii) Adherence data. Patients were supplied with one MEMS-capped bottle for the tenofovir disoproxil fumarate/emtricitabine fixed-dose combination tablets, which recorded the exact time of each opening of the caps. In addition, patients were asked to note any deviations from the MEMS-recorded data. MEMS-recorded times were compared to patients' reports of the previous dose intake. When discrepancies between MEMS-recorded and patient-reported intake prior to sampling were observed (>3 h), the MEMS-reported time was kept. In the case of missing MEMS records, when the sampled concentration level was deemed consistent with an observant drug intake, intake times prior to the sampling occasion were imputed to theoretical values. This method is similar to the one used for modeling atazanavir and ritonavir PK of the same patients using their corresponding MEMS (29).

(iv) Pharmacogenetic data. Three genetic polymorphisms were studied: *ABCC2* (rs717620), *ABCC4* (rs1751034), and *ABCB1* (rs1045642). All the genotyping analyses are described in reference 23. As the population was a mixture of Caucasian and African persons, within each group, for each polymorphism, Hardy-Weinberg equilibrium was tested for.

Data analysis. (i) Population pharmacokinetic modeling. All data were analyzed using the nonlinear mixed-effects approach available in Monolix 2020 R1 (http://lixoft.com/products/monolix/). The stochastic approximation expectation maximization method was employed throughout the analysis. Simulations, tests, and plots were performed using the mlxR package version 4.2.0 (see the supplemental material) and R software version 3.6.3.

The population pharmacokinetic models describing the PK of TFV, TFV-DP, FTC, and FTC-TP were written as a system of concentration-based equations, thanks to the transformation to micromoles per liter of both plasma and intracellular concentrations described above.

The individual parameters were assumed to be log-normally distributed, and proportional error was employed for description of residual variability. Interindividual variability was explored for all parameters and interoccasion variability for apparent clearance.

The model building procedure was guided by Bayesian information criteria (BIC), residual error standard deviations, relative standard errors, and diagnostic plots.

(ii) Pharmacogenetic and demographic covariate analyses. For the three genetic polymorphisms, we considered an allele dosage model. The demographic covariates gender, weight, race, and age were available, as well as the biological covariate creatinine and the pharmacological covariate atazanavir clearance. Creatinine clearance was calculated using the formula of Cockcroft and Gault (48), and atazanavir clearance was calculated using empirical Bayes estimates from the model accounting for MEMS information developed in reference 23.

Missing continuous covariates were replaced with the median, and patients with missing discrete covariates were discarded from analysis.

Covariate selection for model building was performed using the COSSAC (conditional sampling use for stepwise approach based on correlation tests) procedure, available in the Monolix software. This method alternates between forward and backward covariate selection, depending on the results of correlation tests (Pearson's correlation test for continuous covariates and analysis of variance [ANOVA] for categorical ones). These are calculated with samples from the *a posteriori* conditional distribution. Acceptance and reject of a relationship are based on BIC (49).

(iii) Model simulations. Using the combined model population parameter estimates, we simulated PK profiles of TFV, TFV-DP, FTC, and FTC-TP for 1,000 subjects following a 7-day-a-week regimen (as in the ANRS 134-COPHAR 3 trial) or a 4-consecutive-day-a-week regimen over 12 weeks (as in the ANRS 162-4D trial) assuming perfect adherence and derived the 10th, 50th, and 90th predicted percentiles.

Using these simulations, we derived C_{avg} and C_{min} as the average and predose concentrations from week 4 to the last observation according to dosing history and over a 2-week window at steady state assuming perfect adherence, to characterize exposure in patients experiencing successful viral suppression at steady state.

SUPPLEMENTAL MATERIAL

Supplemental material is available online only.

SUPPLEMENTAL FILE 1, DOCX file, 0.01 MB.

ACKNOWLEDGMENTS

We thank the ANRS for funding this research.

We thank all the patients who participated in the ANRS 134-COPHAR 3 trial as well as their health care providers.

We declare no conflict of interest.

J.B. and L.F. analyzed the data and wrote the manuscript; F.M., A.B.-T., C.G., and A.-M.T. wrote the protocol and reviewed the manuscript; A.B.-T., C.B., and A.P. supervised drug assays and reviewed the manuscript; C.V. performed the pharmacogenetic analyses and reviewed the manuscript; R.S. and E.T. performed the research and reviewed the manuscript.

The ANRS 134-COPHAR 3 study group includes the following: scientific committee: A. Barrail-Tran, A. Brunet, M.-J. Commoy, S. Couffin-Cadiergues, D. Descamps, X. Duval, C. Goujard, C. Le Guellec, F. Mentré, G. Nembot, A.-M. Taburet, B. Vrijens; clinical centers: Ajana, Aissi, Baclet, Besnier, Bollens, Boulanger, Brochier, Brunet, Chaix, Ciuchete, Ghosn, Duval, Ferret, Ferret, Gaubin, Goujard, Girard, Kouadio, Lupin, Parienti, Parrinello, Poinçon de la Blanchardière, May, Marien, Medintzeff, Metivier, Mole, Molina, Nau, Ouazene, Pintado, Quertainmont, Ramani, Rami, Sellier, Simon, Talbi, Thoirain, Verdon, Trépo, Wassoumbou, Yazdanpanah; pharmacological centers: Barrail-Tran, Gagneux, Delhotal, Hoizey, Houdret, Leguellec, Peytavin, Poirier, Sauvageon, Taburet; virological centers: André, Soulié, Calvez, Morand-Joubert, Harchi, Bocket, Mourez, Palmer, Pallier, Deschamps, Mazeron, Bolmann, Storto, Thanh Thuy; monitoring: G. Nembot, G. Unal, F. Mentré; statistical analysis: F. Mentré, X. Panhard, R. Savic, B. Vrijens.

REFERENCES

1. WHO. 2021. Consolidated guidelines on HIV prevention, testing, treatment, service delivery and monitoring: recommendations for a public health approach. World Health Organization, Geneva, Switzerland. http://www.ncbi.nlm.nih.gov/books/NBK572729/.
2. Eke AC, Shoji K, Best BM, Momper JD, Stek AM, Cressey TR, Mirochnick M, Capparelli EV. 2021. Population pharmacokinetics of tenofovir in pregnant and postpartum women using tenofovir disoproxil fumarate. Antimicrob Agents Chemother 65:e02168-20.
3. Dickinson L, Gurjar R, Stöhr W, Bonora S, Owen A, D'Avolio A, Cursley A, Molina J-M, Fäetkenheuer G, Vandekerckhove L, Di Perri G, Pozniak A, Richert L, Raffi F, Boffito M, NEAT001/ANRS143 Study Group. 2020. Population pharmacokinetics and pharmacogenetics of ritonavir-boosted darunavir in the presence of raltegravir or tenofovir disoproxil fumarate/emtricitabine in HIV-infected adults and the relationship with virological response: a sub-study of the NEAT001/ANRS143 randomized trial. J Antimicrob Chemother 75:628–639. https://doi.org/10.1093/jac/dkz479.
4. Stranix-Chibanda L, Anderson PL, Kacanek D, Hosek S, Huang S, Nematadzira TG, Taulo F, Korutaro V, Nakabiito C, Masenya M, Lypen K, Brown E, Ibrahim M, Yager J, Wiesner L, Johnston B, Amico KR, Rooney JF, Chakhtoura N, Spiegel HML, Chi BH, IMPAACT 2009 Team. 2021. Tenofovir diphosphate concentrations in dried blood spots from pregnant and postpartum adolescent and young women receiving daily observed pre-exposure prophylaxis in sub-Saharan Africa. Clin Infect Dis 73:e1893–e1900. https://doi.org/10.1093/cid/ciaa1872.
5. Tanaudommongkon A, Chaturvedula A, Hendrix CW, Fuchs EJ, Shieh E, Bakshi RP, Marzinke MA. 2022. Population pharmacokinetics of tenofovir, emtricitabine and intracellular metabolites in transgender women. Br J Clin Pharmacol 88:3674–3682. https://doi.org/10.1111/bcp.15310.
6. Duwal S, Sunkara V, von Kleist M. 2016. Multiscale systems-pharmacology pipeline to assess the prophylactic efficacy of NRTIs against HIV-1. CPT Pharmacomet Syst Pharmacol 5:377–387. https://doi.org/10.1002/psp4.12095.
7. Chen X, Seifert SM, Castillo-Mancilla JR, Bushman LR, Zheng JH, Kiser JJ, MaWhinney S, Anderson PL. 2016. Model linking plasma and intracellular tenofovir/emtricitabine with deoxynucleoside triphosphates. PLoS One 11:e0165505. https://doi.org/10.1371/journal.pone.0165505.
8. Anderson PL, Liu AY, Castillo-Mancilla JR, Gardner EM, Seifert SM, McHugh C, Wagner T, Campbell K, Morrow M, Ibrahim M, Buchbinder S, Bushman LR, Kiser JJ, MaWhinney S. 2018. Intracellular tenofovir-diphosphate and emtricitabine-triphosphate in dried blood spots following directly observed therapy. Antimicrob Agents Chemother 62:e01710-17.
9. Rajoli RKR, Demkovich ZR, Flexner C, Owen A, Siccardi M. 2020. Predicting pharmacokinetics of a tenofovir alafenamide subcutaneous implant using physiologically based pharmacokinetic modelling. Antimicrob Agents Chemother 64:e00155-20.
10. Garcia-Cremades M, Vučićević K, Hendrix CW, Jayachandran P, Jarlsberg L, Grant R, Celum CL, Martin M, Baeten JM, Marrazzo J, Anderson P, Choopanya K, Vanichseni S, Glidden DV, Savic RM. 2022. Characterizing HIV-preventive, plasma tenofovir concentrations—a pooled participant-level data analysis from human immunodeficiency virus preexposure prophylaxis clinical trials. Clin Infect Dis 75:1873–1882. https://doi.org/10.1093/cid/ciac313.
11. Rungtivasuwan K, Avihingsanon A, Thammajaruk N, Mitruk S, Burger DM, Ruxrungtham K, Sukasem C, Punyawudho B. 2017. Pharmacogenetics-based population pharmacokinetic analysis of tenofovir in Thai HIV-infected patients. Pharmacogenomics 18:1481–1490. https://doi.org/10.2217/pgs-2017-0128.
12. Nishijima T, Komatsu H, Higasa K, Takano M, Tsuchiya K, Hayashida T, Oka S, Gatanaga H. 2012. Single nucleotide polymorphisms in ABCC2 associate with tenofovir-induced kidney tubular dysfunction in Japanese patients with HIV-1 infection: a pharmacogenetic study. Clin Infect Dis 55:1558–1567. https://doi.org/10.1093/cid/cis772.
13. Moss DM, Neary M, Owen A. 2014. The role of drug transporters in the kidney: lessons from tenofovir. Front Pharmacol 5:248. https://doi.org/10.3389/fphar.2014.00248.
14. Anderson PL, Lamba J, Aquilante CL, Schuetz E, Fletcher CV. 2006. Pharmacogenetic characteristics of indinavir, zidovudine, and lamivudine therapy in HIV-Infected adults: a pilot study. J Acquir Immune Defic Syndr 42:441–449. https://doi.org/10.1097/01.qai.0000225013.53568.69.
15. Rungtivasuwan K, Avihingsanon A, Thammajaruk N, Mitruk S, Burger DM, Ruxrungtham K, Punyawudho B, Pengsuparp T. 2015. Influence of ABCC2 and ABCC4 polymorphisms on tenofovir plasma concentrations in Thai HIV-infected patients. Antimicrob Agents Chemother 59:3240–3245. https://doi.org/10.1128/AAC.04930-14.
16. Cheli S, Baldelli S, De Silvestri A, Fusi M, Minisci D, Gervasoni C, Cattaneo D, Clementi E, Meraviglia P, Montrasio C. 2021. ABCC4 single-nucleotide polymorphisms as markers of tenofovir disoproxil fumarate-induced kidney impairment. Pharmacogenomics J 21:586–593. https://doi.org/10.1038/s41397-021-00235-7.
17. Kiser JJ, Aquilante CL, Anderson PL, King TM, Carten ML, Fletcher CV. 2008. Clinical and genetic determinants of intracellular tenofovir diphosphate concentrations in HIV-infected patients. J Acquir Immune Defic Syndr 1999 47:298–303. https://doi.org/10.1097/QAI.0b013e31815e7478.
18. Neumanova Z, Cerveny L, Ceckova M, Staud F. 2014. Interactions of tenofovir and tenofovir disoproxil fumarate with drug efflux transporters ABCB1, ABCG2, and ABCC2; role in transport across the placenta. AIDS 28:9–17. https://doi.org/10.1097/QAD.0000000000000112.
19. Decloedt EH, Sinxadi PZ, Wiesner L, Joska JA, Haas DW, Maartens G. 2021. Pharmacogenetics of tenofovir and emtricitabine penetration into cerebrospinal fluid. South Afr J HIV Med 22:1206. https://doi.org/10.4102/sajhivmed.v22i1.1206.
20. Hoffmeyer S, Burk O, von Richter O, Arnold HP, Brockmöller J, Johne A, Cascorbi I, Gerloff T, Roots I, Eichelbaum M, Brinkmann U. 2000. Functional polymorphisms of the human multidrug-resistance gene: multiple sequence variations and correlation of one allele with P-glycoprotein expression and activity in vivo. Proc Natl Acad Sci U S A 97:3473–3478. https://doi.org/10.1073/pnas.97.7.3473.
21. Verstuyft C, Schwab M, Schaeffeler E, Kerb R, Brinkmann U, Jaillon P, Funck-Brentano C, Becquemont L. 2003. Digoxin pharmacokinetics and MDR1 genetic polymorphisms. Eur J Clin Pharmacol 58:809–812. https://doi.org/10.1007/s00228-003-0567-5.
22. Gini J, Olagunju A, Dickinson L, Waitt C, Neary M, Else LJ, Siccardi M, Khoo S. 2019. Impact of pharmacogenetics and pregnancy on tenofovir and emtricitabine pharmacokinetics. Pharmacogenomics 20:217–223. https://doi.org/10.2217/pgs-2018-0111.
23. Savic RM, Barrail-Tran A, Duval X, Nembot G, Panhard X, Descamps D, Verstuyft C, Vrijens B, Taburet A-M, Goujard C, Mentré F, ANRS 134–COPHAR 3 Study Group. 2012. Effect of adherence as measured by MEMS, ritonavir boosting, and CYP3A5 genotype on atazanavir pharmacokinetics in treatment-naive HIV-infected patients. Clin Pharmacol Ther 92:575–583. https://doi.org/10.1038/clpt.2012.137.
24. Landman R, de Truchis P, Assoumou L, Lambert S, Bellet J, Amat K, Lefebvre B, Allavena C, Katlama C, Yazdanpanah Y, Molina J-M, Petrov-Sanchez V, Gibowski S, Alvarez JC, Leibowitch J, Capeau J, Fellahi S, Duracinsky M, Morand-Joubert L, Costagliola D, Alvarez J-C, Girard P-M, ANRS 170 QUATUOR study group. 2022. A 4-days-on and 3-days-off maintenance treatment strategy for adults with HIV-1 (ANRS 170 QUATUOR): a randomised, open-label, multicentre, parallel, non-inferiority trial. Lancet HIV 9:e79–e90. https://doi.org/10.1016/S2352-3018(21)00300-3.
25. Duwal S, von Kleist M. 2016. Top-down and bottom-up modeling in system pharmacology to understand clinical efficacy: an example with NRTIs of HIV-1. Eur J Pharm Sci 94:72–83. https://doi.org/10.1016/j.ejps.2016.01.016.
26. Duwal S, Schütte C, von Kleist M. 2012. Pharmacokinetics and pharmacodynamics of the reverse transcriptase inhibitor tenofovir and prophylactic efficacy against HIV-1 infection. PLoS One 7:e40382. https://doi.org/10.1371/journal.pone.0040382.
27. Valade E, Tréluyer J-M, Illamola SM, Bouazza N, Foissac F, De Sousa Mendes M, Lui G, Chenevier-Gobeaux C, Suzan-Monti M, Rouzioux C, Assoumou L, Viard J-P, Hirt D, Urien S, Ghosn J, Evarist ANRS-EP 49 Study Group. 2015. Emtricitabine seminal plasma and blood plasma population pharmacokinetics in HIV-infected men in the EVARIST ANRS-EP 49 Study. Antimicrob Agents Chemother 59:6800–6806. https://doi.org/10.1128/AAC.01517-15.
28. Hirt D, Ekouévi DK, Pruvost A, Urien S, Arrivé E, Blanche S, Avit D, Amani-Bosse C, Nyati M, Legote S, Ek ML, Say L, McIntyre J, Dabis F, Tréluyer J-M. 2011. Plasma and intracellular tenofovir pharmacokinetics in the neonate (ANRS 12109 trial, step 2). Antimicrob Agents Chemother 55:2961–2967. https://doi.org/10.1128/AAC.01377-10.
29. Podany AT, Bares SH, Havens J, Dyavar SR, O'Neill J, Lee S, Fletcher CV, Swindells S, Scarsi KK. 2018. Plasma and intracellular pharmacokinetics of tenofovir in patients switched from tenofovir disoproxil fumarate to tenofovir alafenamide. AIDS Lond Engl 32:761–765. https://doi.org/10.1097/QAD.0000000000001744.
30. Tong L, Phan TK, Robinson KL, Babusis D, Strab R, Bhoopathy S, Hidalgo IJ, Rhodes GR, Ray AS. 2007. Effects of human immunodeficiency virus protease inhibitors on the intestinal absorption of tenofovir disoproxil fumarate in vitro. Antimicrob Agents Chemother 51:3498–3504. https://doi.org/10.1128/AAC.00671-07.
31. Cihlar T, Ray AS, Laflamme G, Vela JE, Tong L, Fuller MD, Roy A, Rhodes GR. 2007. Molecular assessment of the potential for renal drug interactions

between tenofovir and HIV protease inhibitors. Antivir Ther 12:267–272. https://doi.org/10.1177/135965350701200211.
32. Cressey TR, Avihingsanon A, Halue G, Leenasirimakul P, Sukrakanchana PO, Tawon Y, Jaisieng N, Jourdain G, Podany AT, Fletcher CV, Klinbuayaem V, Bowonwatanuwong C. 2015. Plasma and intracellular pharmacokinetics of tenofovir disoproxil fumarate 300 mg every 48 hours vs 150 mg once daily in HIV-infected adults with moderate renal function impairment. Clin Infect Dis 61:633–639. https://doi.org/10.1093/cid/civ346.
33. Dumond JB, Bay CP, Nelson JAE, Davalos A, Edmonds A, De Paris K, Sykes C, Anastos K, Sharma R, Kassaye S, Tamraz B, French AL, Gange S, Ofotokun I, Fischl MA, Vance DE, Adimora AA. 2020. Intracellular tenofovir and emtricitabine concentrations in younger and older women with HIV receiving tenofovir disoproxil fumarate/emtricitabine. Antimicrob Agents Chemother 64:e00177-20.
34. Lu Y, Goti V, Chaturvedula A, Haberer JE, Fossler MJ, Sale ME, Bangsberg D, Baeten JM, Celum CL, Hendrix CW. 2016. Population pharmacokinetics of tenofovir in HIV-1-uninfected members of serodiscordant couples and effect of dose reporting methods. Antimicrob Agents Chemother 60:5379–5386. https://doi.org/10.1128/AAC.00559-16.
35. Punyawudho B, Thammajaruk N, Thongpeang P, Matthews G, Lewin SR, Burger D, Ruxrungtham K, Avihingsanon A. 2015. Population pharmacokinetics of tenofovir in HIV/HBV co-infected patients. Int J Clin Pharmacol Ther 53:947–954. https://doi.org/10.5414/CP202386.
36. Baheti G, Kiser JJ, Havens PL, Fletcher CV. 2011. Plasma and intracellular population pharmacokinetic analysis of tenofovir in HIV-1-infected patients. Antimicrob Agents Chemother 55:5294–5299. https://doi.org/10.1128/AAC.05317-11.
37. Jullien V, Tréluyer J-M, Rey E, Jaffray P, Krivine A, Moachon L, Lillo-Le Louet A, Lescoat A, Dupin N, Salmon D, Pons G, Urien S. 2005. Population pharmacokinetics of tenofovir in human immunodeficiency virus-infected patients taking highly active antiretroviral therapy. Antimicrob Agents Chemother 49:3361–3366. https://doi.org/10.1128/AAC.49.8.3361-3366.2005.
38. Valade E, Tréluyer JM, Bouazza N, Ghosn J, Foissac F, Benaboud S, Fauchet F, Viard JP, Urien S, Hirt D. 2014. Population pharmacokinetics of emtricitabine in HIV-1-infected adult patients. Antimicrob Agents Chemother 58:2256–2261. https://doi.org/10.1128/AAC.02058-13.
39. Ma B, Barth A, McHale CM, Lai MT. 2018. Establishment of intracellular tenofovir-diphosphate as the key determinant for in vitro-in vivo translation of antiviral efficacy. Antiviral Res 151:1–3. https://doi.org/10.1016/j.antiviral.2018.01.005.
40. BREATHER (PENTA 16) Trial Group. 2016. Weekends-off efavirenz-based antiretroviral therapy in HIV-infected children, adolescents, and young adults (BREATHER): a randomised, open-label, non-inferiority, phase 2/3 trial. Lancet HIV 3:e421–e430. https://doi.org/10.1016/S2352-3018(16)30054-6.
41. Abe E, Assoumou L, de Truchis P, Amat K, Gibowski S, Gras G, Bellet J, Saillard J, Katlama C, Costagliola D, Girard PM, Landman R, Alvarez JC. 2021. Pharmacological data of a successful 4-days-a-week regimen in HIV antiretroviral therapy (ANRS 162-4D trial). Br J Clin Pharmacol 87:1930–1939. https://doi.org/10.1111/bcp.14586.
42. Podany A, Bares SH, Havens J, Shetty RD, O'Neill J, Lee S, Fletcher C, Swindells S, Scarsi KK. 2017. Plasma and intracellular PK of tenofovir in patients switched from TDF to TAF, abstr 408. Conf Retrovir Opportunistic Infect. http://www.croiconference.org/sessions/plasma-and-intracellular-pk-tenofovir-patients-switched-tdf-taf.
43. Cottrell ML, Garrett KL, Prince HMA, Sykes C, Schauer A, Emerson CW, Peery A, Rooney JF, McCallister S, Gay C, Kashuba ADM. 2017. Single-dose pharmacokinetics of tenofovir alafenamide and its active metabolite in the mucosal tissues. J Antimicrob Chemother 72:1731–1740. https://doi.org/10.1093/jac/dkx064.
44. Le Saux T, Chhun S, Rey E, Launay O, Weiss L, Viard J-P, Pons G, Jullien V. 2008. Quantification of seven nucleoside/nucleotide reverse transcriptase inhibitors in human plasma by high-performance liquid chromatography with tandem mass-spectrometry. J Chromatogr B Analyt Technol Biomed Life Sci 865:81–90. https://doi.org/10.1016/j.jchromb.2008.02.008.
45. Pruvost A, Théodoro F, Agrofoglio L, Negredo E, Bénech H. 2008. Specificity enhancement with LC-positive ESI-MS/MS for the measurement of nucleotides: application to the quantitative determination of carbovir triphosphate, lamivudine triphosphate and tenofovir diphosphate in human peripheral blood mononuclear cells. J Mass Spectrom 43:224–233. https://doi.org/10.1002/jms.1294.
46. Chapman EH, Kurec AS, Davey FR. 1981. Cell volumes of normal and malignant mononuclear cells. J Clin Pathol 34:1083–1090. https://doi.org/10.1136/jcp.34.10.1083.
47. Segel GB, Cokelet GR, Lichtman MA. 1981. The measurement of lymphocyte volume: importance of reference particle deformability and counting solution tonicity. Blood 57:894–899. https://doi.org/10.1182/blood.V57.5.894.894.
48. Cockcroft DW, Gault MH. 1976. Prediction of creatinine clearance from serum creatinine. Nephron 16:31–41. https://doi.org/10.1159/000180580.
49. Ayral G, Si Abdallah JF, Magnard C, Chauvin J. 2021. A novel method based on unbiased correlations tests for covariate selection in nonlinear mixed effects models: the COSSAC approach. CPT Pharmacomet Syst Pharmacol 10:318–329. https://doi.org/10.1002/psp4.12612.